In-situ, real time micro-CT imaging of pore scale processes, the next frontier for laboratory based micro-CT scanning

Boone, Marijn[1,2], Bultreys, Tom[2], Masschaele, Bert[1], Van Loo, Denis[1], Van Hoorebeke, Luc[3], Cnudde, Veerle[2]
[1]X-Ray Engineering bvba
[2]UGCT/PProGRess, Dept. of Geology, Ghent University
[3]UGCT, Dept. of physics and astronomy, Ghent University

This paper was prepared for presentation at the International Symposium of the Society of Core Analysts held in Snowmass, Colorado, USA, 21-26 August 2016

ABSTRACT

Over the past decade, laboratory based X-ray computed micro-tomography (micro-CT) has given unique insights in the internal structure of complex reservoir rocks, improving the understanding of pore scale processes and providing crucial information for pore scale modelling. Especially in-situ imaging using X-ray optimized Hassler type cells has enabled the direct visualization of fluid distributions at the pore scale under reservoir conditions. While sub-micrometre spatial resolutions are achievable in lab-based micro-CT, the temporal resolutions are still limited to minutes or hours. This time restriction is often a bottleneck for imaging dynamic in-situ processes, thus limiting the applicability to relatively slow pore scale processes occurring in the order of hours to days, or to end points in drainage-imbibition cycles.

To overcome this issue, X-ray Engineering (XRE) and Ghent University's Centre for X-ray Tomography (UGCT) have jointly developed a gantry-based micro-CT system. This system's X-ray tube and detector rotate continuously in a horizontal plane around the fixed sample. The setup still allows to tune the geometrical magnification, with spatial resolutions down to 5 μm. This fixed sample setup is also ideal for in-situ imaging, as the flow cells can be directly connected to high pressure flow tubing and sensor lines, without the need to allow rotational movement relative to the X-ray source and detector. An efficient hardware design with a fast flat panel detector, combined with custom X-ray transparent flow cells to increase X-ray flux and dedicated 4D software tools in acquisition, reconstruction and analysis, allows to reach temporal resolutions in the order of seconds.

The possibilities of this new approach in dynamic in-situ imaging are illustrated with flow tests on a carbonate sample. We discuss the challenges in dynamic imaging and present methods to improve X-ray flux and optimize image quality by means of this experiment. Furthermore, we show that the integration of fast imaging experiments with other information from peripheral sensors or from imaging data at different resolutions can help to link behaviour at the pore scale to the effective properties at the core scale, but also facilitates the experimental workflow.

INTRODUCTION

X-ray computed microtomography (micro-CT) has the unique ability to obtain reliable high resolution 3D information inside otherwise non-transparent objects in a non-destructive manner. Over the past 2 decades micro-CT evolved from a synchrotron technique to a standard laboratory microscopy technique. In this period, the achievable spatial resolution of the laboratory based micro-CT systems has improved drastically, reaching resolutions up to 50nm for some systems. This evolution has had important implications in the field of geosciences, as it enabled detailed microscopic studies of the internal structure of geological samples in 3D, while before this was limited to 2D techniques like optical or scanning electron microscopy. It was especially challenging to describe the pore space of a rock, which is essentially a 3D property of a rock, and therefore required statistical or process based modelling to extrapolate the 2D information to a 3D model [1]. The evolution in micro-CT imaging enabled the direct visualization and characterization of the pore space in 3D at scales below the micrometer, even for complex carbonate pore systems.

Besides the static pore structure characterization, the non-destructive nature of micro-CT also makes it possible to visualize different fluids inside the pore space and to monitor how these fluids migrate through the rock. This is in recent years often referred to as in-situ micro-CT and implies the imaging of a sample under certain well-constrained external conditions [2-8]. In pore scale studies these conditions are usually increased pressure and temperature in order to obtain an insight in for example reactive flow, multiphase flow and rock mechanics under reservoir conditions. Traditional flow studies at reservoir conditions are performed by placing reservoir samples in large stainless steel Hassler type flow cells and monitoring the fluid transport through the samples using different sensors (e.g. pressure, pH and electrical conductivity) and analyzing the chemical composition of the fluid coming in and going out the cell. Based on the information of these different sensors and chemical data, assumptions are made on the pore scale processes occurring in the sample. However, what happens inside individual pores in the sample remains inaccessible. In-situ micro-CT imaging makes it possible to visualize fluid distribution in the pore space and if and how the pore structure of the rock changes throughout the experiment.

Traditional Hassler type flow cells are however not practical for in-situ imaging due to their size and constitution. An in-situ set-up for X-ray imaging requires a custom built, miniature version of a traditional Hassler type cell. The first requirement of such a custom built is the diameter of the cell. This diameter has to be kept as small as possible, as most laboratory based micro-CT systems use a geometrical magnification to obtain high resolutions. The second requirement is the composition of the cell. The cell needs to be made from X-ray transparent materials, in order to ensure that a sufficient X-ray flux reaches the detector. These in-situ cells are therefore usually constructed out of weakly X-ray attenuating metals like aluminium [9] or strong polymers like PEEK[9] or carbon fiber [8,11,12] fiber instead of stainless steel.

When a fluid is injected into a reservoir sample in an in-situ setup, the fluid moves trough the pore space and can interact with other fluids in the pore space or with the rock itself. By monitoring these interactions over time using micro-CT imaging it is possible to

capture the dynamics of pore scale processes. In-situ imaging is therefore often related to dynamic or 4D (3D + time) imaging. However, to acquire reliable pore scale 3D images, the sample needs to remain unchanged during the micro-CT acquisition, otherwise motion artefacts and image blurring can occur. To avoid these motion artefacts, the temporal resolution of the micro-CT system should be high enough to capture the dynamic changes occurring inside the sample while maintaining e.g. flow conditions. While the spatial resolution of laboratory micro-CT system has improved during the last years, the temporal resolution has remained in the order of minutes to hours. This limits the type of pore scale processes that can be visualized using traditional laboratory micro-CT systems to slow processes (hours to days), like mineral-fluid interactions in CCS studies [13], or to quasi-static fluid distributions during drainage-imbibition cycles [14]. Monitoring fast (seconds to minutes) pore scale processes mostly remained restricted to synchrotron facilities where temporal resolutions below 1 second can be obtained.

To tackle this issue, we have developed a benchtop scale gantry-based micro-CT system which is optimized for dynamic in-situ imaging of pore scale processes (figure 1). The temporal resolution of the system is around 12 seconds, which is an order of magnitude higher compared to standard micro-CT systems. This is illustrated in figure 2, where an overview of the spatial and temporal resolution of laboratory and synchrotron based micro-CT systems is given.

In this manuscript the possibilities of this gantry-based micro-CT system are illustrated by a solute transport experiment using a tracer salt inside a carbonate sample. Traditionally, a tracer salt would be pumped through the sample (while mounted in a flow cell) and the conductivity at the outlet would be monitored. Based on these measurements one can investigate the dispersive behavior of the porous sample, and determine if the transport of a solute through the sample is dominated by advective or diffusive processes. Here we augment this data by directly visualizing – spatially resolved - how the tracer salt is moving through the pore space of the carbonate.

While this is an example of single phase flow visualization, dynamic in-situ imaging is also applicable to multiphase flow. As an example of fast pore scale imaging of multiphase flow, Bultreys et al. (2015) presented the visualization of Haines jumps in a sandstone sample with the same laboratory setup as used this work[16].

Experimental setup and optimizations for dynamic imaging

For the in-situ solute transport experiment a simple flow cell with confining pressure was used (figure 1). Because this experiment is conducted at low pressure conditions, the used flow cell was constructed out of polymethylmethacrylate (PMMA), which can be considered as quasi transparent for X-rays, especially in comparison to the carbonate sample. In the flow cell, a carbonate sample of 6 mm diameter and 16 mm in height was mounted in a viton sleeve. A confining pressure of 10 bar was placed around the sleeve using a manual syringe pump. A MilliGAT high-precision continuous flow pump controlled the flow through the sample. To the outlet of the cell an electrical conductivity sensor was placed as an indication to the brine salinity. The diameter of the entire flow cell is 25 mm, allowing to obtain a spatial resolution of 7 μm and a field of view which covers the entire diameter of the carbonate sample.

The carbonate sample investigated in this experiment was the Savonnières limestone, which has a porosity ranging from 22% to 40% and a permeability from 115 to more than 2000 mD, depending on local variations [20]. It is a grain supported oolithic limestone consisting of ooids and shell fragments which are overgrown by sparite. During diagenesis, some grain fragments were partially dissolved, resulting in a pore network with well-connected pores between the grains (intergranular porosity) and secondary porosity inside the dissolved grains (intragranular porosity or vuggy porosity), which is connected to the rest of the pore network through micropores [17]. A high-quality micro-CT 2D slice through the sample with a resolution of 7.3µm is given in figure 3. The resolution is sufficient to capture the macroporosity in the sample, but unable to capture the microporous connections between some larger pore bodies.

The dried limestone sample was flushed with CO_2 to remove the air phase in the pores. Afterwards the sample was flushed with distilled water for a period of 2 hours to obtain a complete water saturation. Scans before and after water flushing were used to evaluate the water saturation degree and check for potential dissolution effects in the sample due to the CO_2 dissolution in the pore fluid. No dissolution effects were apparent in the CT images at a resolution of 7.3µm. To investigate dispersive solute transport in the sample, a salt solution of 10 wt.% CsCl was injected, because Cs acts as a tracer due to its high X-ray attenuation coefficient. The change of the salt concentration in the outgoing fluid was measured using the conductivity sensor on the in-situ flow cell, while the changes in the distribution of the salt solution in the pore space of the carbonate sample were continuously monitored by dynamic micro-CT imaging. The experiment was performed twice on the same carbonate sample at volumetric injection rates of 0.25 µl/s in the first run and 1 µl/s in the second run (with sufficient clean water flushing in between the runs).

In order to obtain a 3D image of the sample with X-ray micro-CT, radiographs of the sample have to be taken at different angles, which requires a rotation of the sample relatively to the source and detector. The self-developed in-situ cell setup in the described experiment had 2 flowlines going towards the cell (inlet and confining pressure), 1 flowline going out of the sample and 1 sensor wire coming from the sample. A more complex setup often has even more (high pressure) flow and sensor lines connected to the cell, which makes a rotational movements of the cell challenging. For time lapse micro-CT imaging, where scans are acquired at a time interval of typically several hours or days it is possible to perform a full rotation and then return to the original position, causing less problems with fluid or sensor line tangling. Monitoring fast dynamic processes requires a continuous rotation of the in-situ cell setup, which in turn requires very complex in-situ cell designs with slip ring hydraulic/sensor contacts or with integration of pumps in the in-situ cell [18].

The fixed sample configuration in our gantry based setup is ideal as (high pressure) tubing or sensor lines remain immobile, thus avoiding entanglement, vibrations during scanning and possible flow instabilities in the fluids going towards the sample.

The micro-CT systems design is optimized for fast dynamic in-situ imaging[19]. The X-ray source and detector are mounted on a gantry, which can be continuously rotated at a maximum speed of 30°/s or 12 seconds for 360° rotation. Apart from the rotational

movement, the gantry can also perform a translational movement to change the distance between the X-ray source and the detector allowing to tune the geometrical magnification of the sample (figure 1). The X-ray source is a compact closed type transmission source with a maximum tube voltage of 130kV and a maximum power of 39W. The tube has a focal spot of 5 μm, which is also the highest achievable spatial resolution with the system. The detector is a CMOS flat panel with a thick CsI scintillator and a readout speed of 30 frames per second at a full resolution and 60 frames per second in 2 x 2 binned mode. The sample stage can be moved vertically with a travel of 0.75 m. This offers flexibility to mount different types of in-situ equipment, allows to perform stacked scans of elongated core samples for a more representative overview and even follow slow moving fluid fronts through the sample.

Before performing dynamic acquisition, a high-quality 3D image of the pore structure was obtained in a normal acquisition of 30 minutes at a voxel size of 7.3 μm, a 100 kV tube voltage and 6W tube power (figure 3). For the dynamic scan the detector was used in a 2 x 2 binned mode resulting in a voxel size of 14.6 μm and an increase of the signal to noise in the micro-CT image. The tube voltage and tube power were increased to 130 kV and 16 W respectively, to increase the X-ray flux reaching the detector and therefore decrease the noise level in the micro-CT image. The total acquisition time was 15 minutes and each 360 degree rotation took 12 seconds, resulting in a total of 45000 projection images. This data was recorded and processed with the proprietary 4D tools (XRE, Ghent, Belgium) in the ACQUILA software (UGCT/XRE, Ghent, Belgium). Dynamic acquisitions generate a massive amount of data and require dedicated smart reconstruction and analysis tools to the desired and useful information of the pore scale process under investigation. The acquired projections were automatically analysed and differences in radiographies were used to pinpoint changes in the pore space of the sample. Data from external sources like sensor data can also be incorporated and synced with the continuous stream of X-ray projections to augment the data and avoid redundant data from being reconstructed. Tomographic reconstruction was performed with the FDK algorithm, implemented on the GPU.

Because the acquisition was continuous, projections acquired during any full rotation of the system could be reconstructed regardless of the starting angle. This is very useful when discrete events like fracture formation or sudden pore filling events like Haines jumps are visualized, as a reconstruction can be done just before and just after the event. This avoids image blurring and motion artefacts. In these experiments the pore scale process is a continuous process without discrete events. Therefore the angle between every consecutive reconstruction equalled 360 degrees, resulting in a full 3D image every 12 seconds.

RESULTS AND DISCUSSION

The effluent salt concentration was calculated based on the electrical conductivity measurements, resulting in breakthrough curves for both experiments. The two curves for the 0.25 μl/s and the 1 μl/s experiments are shown in figure 4. In the breakthrough curve of the 1 μl/s flow experiment, we can see an almost instantaneous increase in salt concentration of the effluent fluid, indicating that the dispersion in the system is mainly

controlled by advective processes.. We used a non-linear least squares analysis implemented in STANMOD to roughly estimate the dispersion coefficient based on the breakthrough curves. This yielded an effective dispersion coefficient of 3.89E-3 mm^2/s for the 1 µ l/s experiment. Assuming a tortuosity of 24.4 and a porosity of 26% in Savonnières [20], the effective diffusion coefficient of Cs in this rock is estimated at 1.83E-5 mm^2/s. This confirms that the behavior in the well-connected macropores is advection-dominated.

In the 0.25 µl/s constant flow experiment the diffusive processes play a larger role in the dispersion coefficient, but generally it is also an advective dominated system (estimated dispersion coefficient 1.44E-3 mm^2/s). From this curve it is however also clear that the solute transport process takes longer than the scanned timeframe of 15 minutes, so only a part of the process was captured with in-situ dynamic imaging.

Vertical slices trough the reconstructed volumes of the dynamic acquisition are given in figure 5 and figure 6. In the raw vertical slices the Cs-concentration rise within the pore space can be clearly seen. In the 1 µl/s experiment the fluid front reaches the bottom of the sample after about 1 minute and reaches the top about 1 minute later. The heterogeneity of the advective flow field is clearly visible: the Cs-concentration in some well-connected macropores lags behind. After about 3 minutes however, the well-connected pore space is fully saturated with the salt. Some pores in the system behave rather differently and show a significantly slower concentration increase. Most of these pores are ooids that were dissolved during diagenesis of the carbonate and which are only connected to the rest of the pore network through micropores. In these microporous connections, the advective flow of the solute is limited, and the Cs-transport to these pores is thus likely dominated by diffusion. In figure 6 at 168s, the indicated ooid pore is still filled with distilled water, while the rest of the pore space already contains solute. It takes more then 10 minutes for its Cs-concentration starts to rise. It should be noted that in the 1 µl/s experiment, some pores contain trapped air. During the experiment, this can be considered as an immobile phase that does not interact with the solute transport.

In the 0.25 µl/s experiment, the Cs-concentration rise is much slower and moves more gradually towards the top of the sample. Contrary to the 1 µl/s experiment, the well-connected macropores have not yet reached a constant Cs-saturation before the grey values of the ooid pores start increasing. This could indicate that diffusive transport may start to play a role in some parts of the pore space with lower advection rates (other than the ooid pores). Advective transport is however still dominant for the solute distribution at 0.25 µl/s.

It is possible to obtain a good idea about the general type of transport in the carbonate based on the fast scans. The noise level in these images makes it however difficult to obtain reliable quantitative information from the fast scans. Especially segmenting the pore space is a challenging endeavour due to the noise in the data and the changes inside the pores. One of the options to improve the fast micro-CT data is to apply image filtering. For example, 4D filtering seems to be a promising method to deal with the higher noise levels associated with fast-acquired, dynamic data [2,16]. A second method uses high quality, pre-acquired data on the sample to augment the 4D data. For example, in the present case the pore space can be segmented from a high-quality micro-CT scan,

which can then be used as a mask to analyze the dynamic data (figure 3). By analyzing the different phases on the high quality data and combining this information with the fast scans, a dynamic map of the changing pore space can be obtained. Research into the extraction of the velocity field from these experiments is ongoing.
Given the fact that at short ranges in the pore space, the Cs-concentration can be assumed to vary little, we applied a median filter to average the greyscale values in the pore space. The resulting 3D distribution map of the CsCl concentration in the sample in function of time is shown in figure 7 for the 0.25 µl/s experiment. This concentration map shows pores where the CsCl concentration change more slowly in time compared to the surrounding pores. These pores remain blue through time and are the more isolated vuggy ooid porosity, in which the concentration is controlled by mainly diffusive processes. The concentration in the surrounding pores increases more rapidly which is illustrated by the more rapid change from blue to orange-red. These pores are well connected and are the preferred pathways along which the solute is transported.

CONCLUSION

The possibilities of laboratory based in-situ fast dynamic imaging are illustrated by visualizing solute transport inside a porous carbonate rock. By maximizing the X-ray transparency in-situ flow cell; optimizing the X-ray flux from the source; choosing the right detector with a maximum efficiency and high read out speed; optimizing dynamic reconstruction and integrating other micro-CT data to augment the dynamic scans, it is possible to obtain temporal resolutions of 12 seconds. Thus allowing to continuously monitor and quantify dynamic processes pore scale processes through time. In the applied example a 3D map of the solute concentration in function of time could be generated, which allows to visualize advection controlled preferential flow paths and more isolated pore bodies controlled by diffusive transport.
These results provide a direct insight in fluid transport in complex porous media and provide vital information to predict slower processes like reactive fluid flow and provide input and validation for pore scale modeling.

ACKNOWLEDGEMENTS

The Research Foundation – Flanders (FWO) is acknowledged for the FWO research grants 1521815N and 3G004115. Tom Bultreys is funded by the Flemish agency for Innovation by Science and Technology.

REFERENCES

1. Cnudde, V., & Boone, M. N. (2013). High-resolution X-ray computed tomography in geosciences: A review of the current technology and applications. Earth-Science Reviews, 123(0), 1–17.
2. Bultreys, T., Boone, M. A., Boone, M. N., De Schryver, T., Masschaele, B., Van Hoorebeke, L., & Cnudde, V. (2015). Fast laboratory-based micro-computed tomography for pore-scale research: illustrative experiments and perspectives on the future. *Advances in Water Resources, in press*.

3. Rücker M, Berg S, Armstrong RT, Georgiadis A, Ott H, Schwing A, et al. (2015) From connected pathway flow to ganglion dynamics. Geophys Res Lett, 42,3888–94.
4. Armstrong RT, Ott H, Georgiadis A, Rücker M, Schwing A, Berg S. (2014) Subsecond pore-scale displacement processes and relaxation dynamics in multiphase flow. Water Resour Res,50,9162–76.
5. Youssef S, Deschamps H, Dautriat J, Rosenberg E, Oughanem R, Maire E, et al. (2013) 4D Imaging of fluid flow dynamics in natural porous media with ultra-fast X-ray microtomography. Int. Symp. Soc. Core Anal., Napa Valley, USA: Society of Core Analysts.
6. Andrew, M. G., Bijeljic, B., Blunt, M. J. (2013) Pore-scale imaging of geological carbon dioxide storage under in situ conditions. Geophysical Research Letters, 40, 3915–3918.
7. Andrew M, Menke H, Blunt MJ, Bijeljic B. (2015) The Imaging of Dynamic Multiphase Fluid Flow Using Synchrotron-Based X-ray Microtomography at Reservoir Conditions. Transp Porous Media, 110, 1–24.
8. Iglauer S, Paluszny A, Pentland CH, Blunt MJ. (2011) Residual CO2 imaged with X-ray micro-tomography. Geophys Res Lett, 38.
9. Fusseis F, Steeb H, Xiao X, Zhu W, Butler IB, Elphick S, et al. A low-cost Xray-transparent experimental cell for synchrotron-based X-ray microtomography studies under geological reservoir conditions. J Synchrotron Radiat 2014;21:251–3.
10. Boone MA, Nielsen P, De Kock T, Boone MN, Quaghebeur M, Cnudde V. Monitoring of stainless-steel slag carbonation using X-ray computed microtomography. Environ Sci Technol 2014;48:674–80.
11. Andrew M, Bijeljic B, Blunt MJ. Pore-scale imaging of trapped supercritical carbon dioxide in sandstones and carbonates. Int J Greenh Gas Control 2014;22:1–14.
12. Ott H, de Kloe K, van Bakel M, Vos F, van Pelt A, Legerstee P, et al. Core-flood experiment for transport of reactive fluids in rocks. Rev Sci Instrum 2012;83:084501.
13. Herring AL, Harper EJ, Andersson L, Sheppard A, Bay BK, Wildenschild D. (2013) Effect of fluid topology on residual nonwetting phase trapping: Implications for geologic CO2 sequestration. Adv Water Resour, 62, 47–58.
14. Myers GR, Kingston AM, Varslot TK, Turner ML, Sheppard AP. (2011) Dynamic X-ray micro-tomography for real time imaging of drainage and imbibition processes at the pore scale. Int. Symp. Soc. Core Anal., Society of Core Analysts.
15. Maire E, Withers PJ. Quantitative X-ray tomography. Int Mater Rev 2014;59:1–43.
16. Bultreys, T., Boone, M., Boone, M., De Schryver, T., Masschaele, B., Van Loo, D., Van Hoorebeke, L., et al. (2015). Real-time visualization of Haines jumps in sandstone with laboratory-based microcomputed tomography. Water Resources Research, 51(10), 8668–8676.

17. Roels S, Elsene J, Carmeliet J, Hens H. Characterisation of pore structure by combining mercury porosimetry and micrography. Mater Struct 2001;34:76–82.
18. Berg, S., Ott, H., Klapp, S. A., Schwing, A., Neiteler, R., Brussee, N., … Stampanoni, M. (2013). Real-time 3D imaging of Haines jumps in porous media flow. *Proceedings of the National Academy of Sciences*, *110*(10), 3755–3759.
19. Dierick M, Van Loo D, Masschaele B, Van den Bulcke J, Van Acker J, Cnudde V, et al. Recent micro-CT scanner developments at UGCT. Nucl Instrum Methods Phys Res Sect B Beam Interact Mater Atoms 2014;324:35–40.
20. Derluyn, H. (2012) Salt transport and crystallization in porous limestone: neutron – X-ray imaging and poromechanical modeling, Dissertation ETH No. 20673, ETH Zurich, Switzerland.

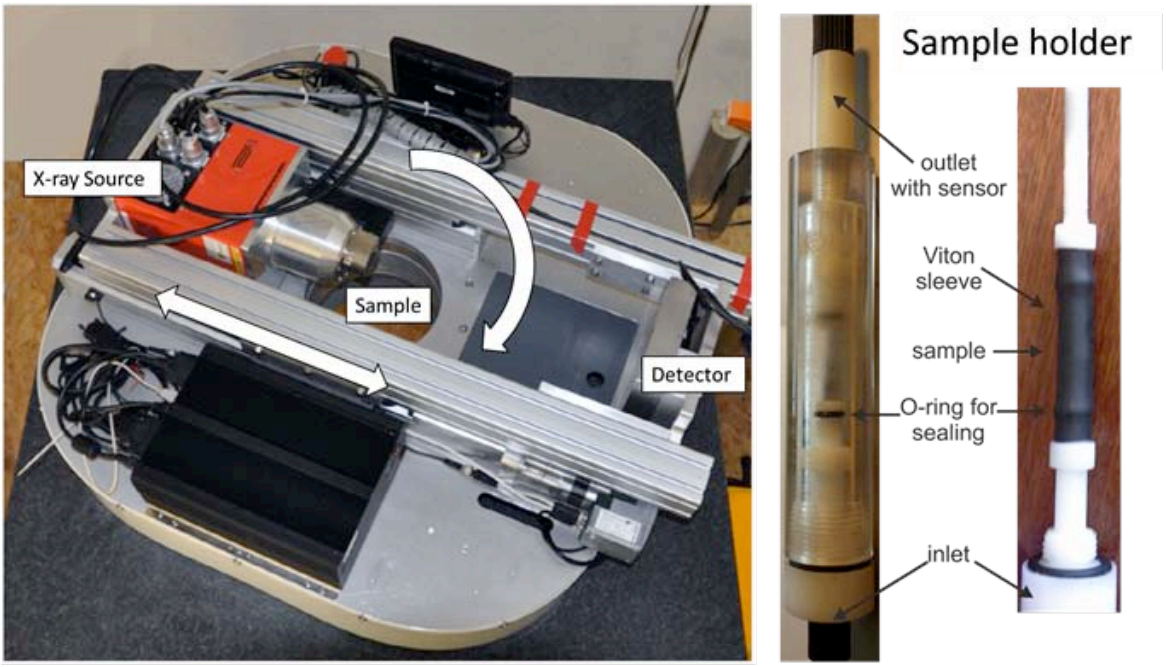

Figure 1. Scanner setup with arrows illustrating the magnification and rotational movement of source and detector (left). Detail of the flow cell (right).

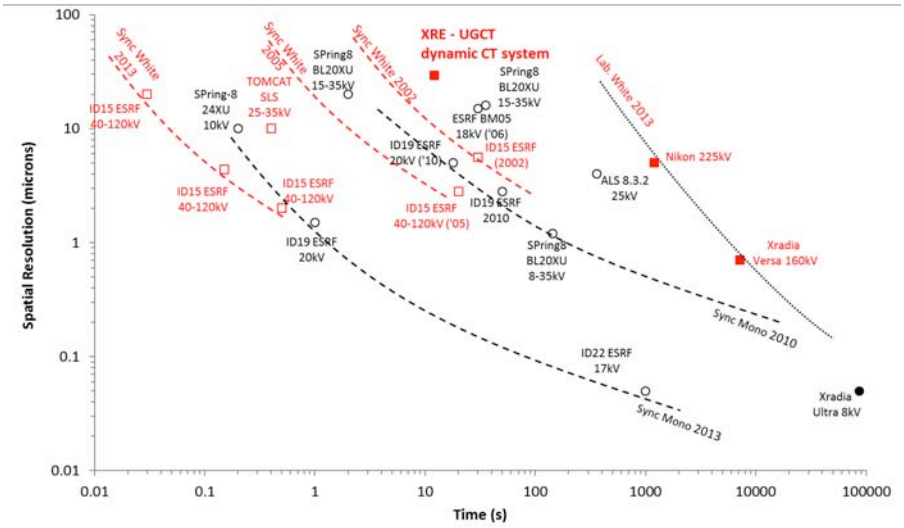

Figure 2. (adapted from [15]) The temporal and spatial resolutions attained at different synchrotron beamlines and lab set-ups. Open symbols denote synchrotron sources, while filled ones represent laboratory sources, squares denote polychromatic ("white") beam and circles denote monochromatic scanners. The reported time is the time needed to gather 1000 projections

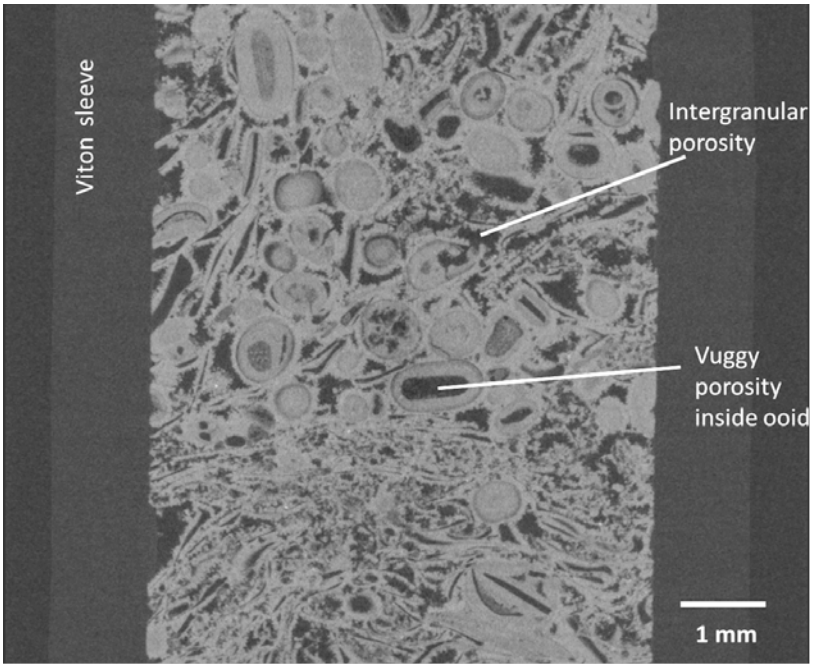

Figure 3. Vertical slice through a high quality scan of the Savonnières carbonate sample showing the inter- and intragranular porosity in the sample. Scan time 30 minutes and resolution 7.3 µm.

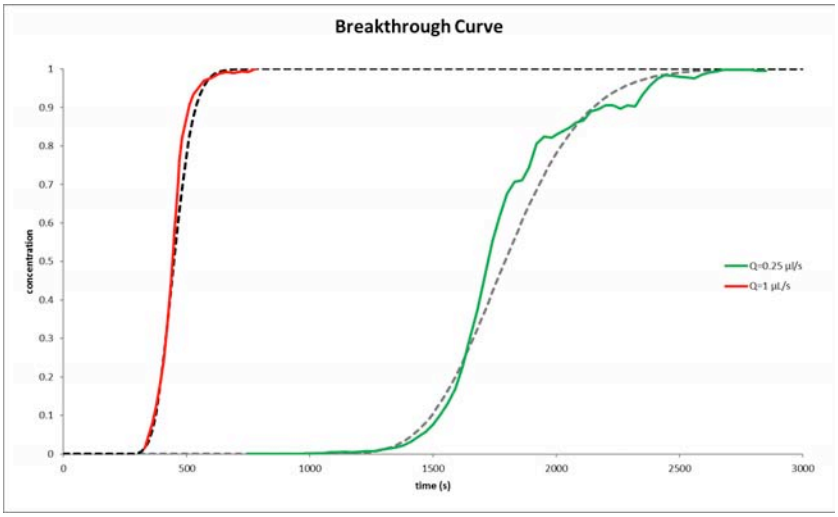

Figure 4. Breakthrough curve of the salt solution determined by conductivity measurement in the flow cell

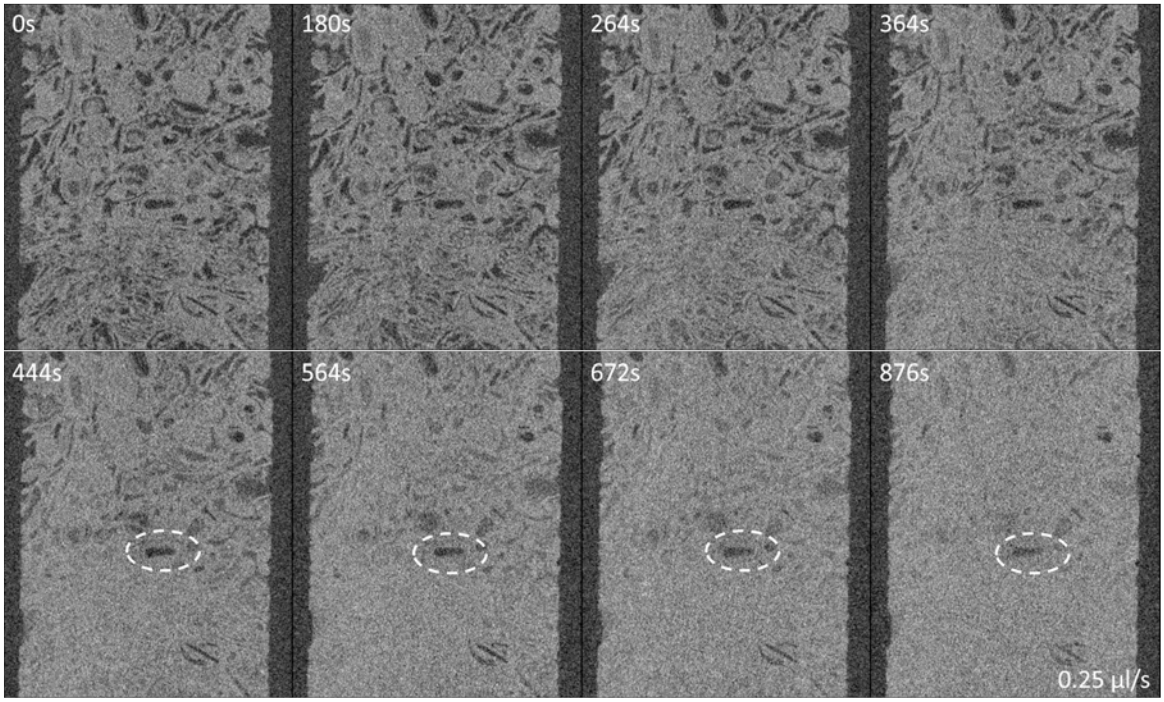

Figure 5. Raw vertical slices through selected reconstructed volume of the continuous acquisition. Experiment at a constant flow speed of 0.25 µ l/s. Dotted circle indicating more isolated, diffusion controlled vuggy porosity.

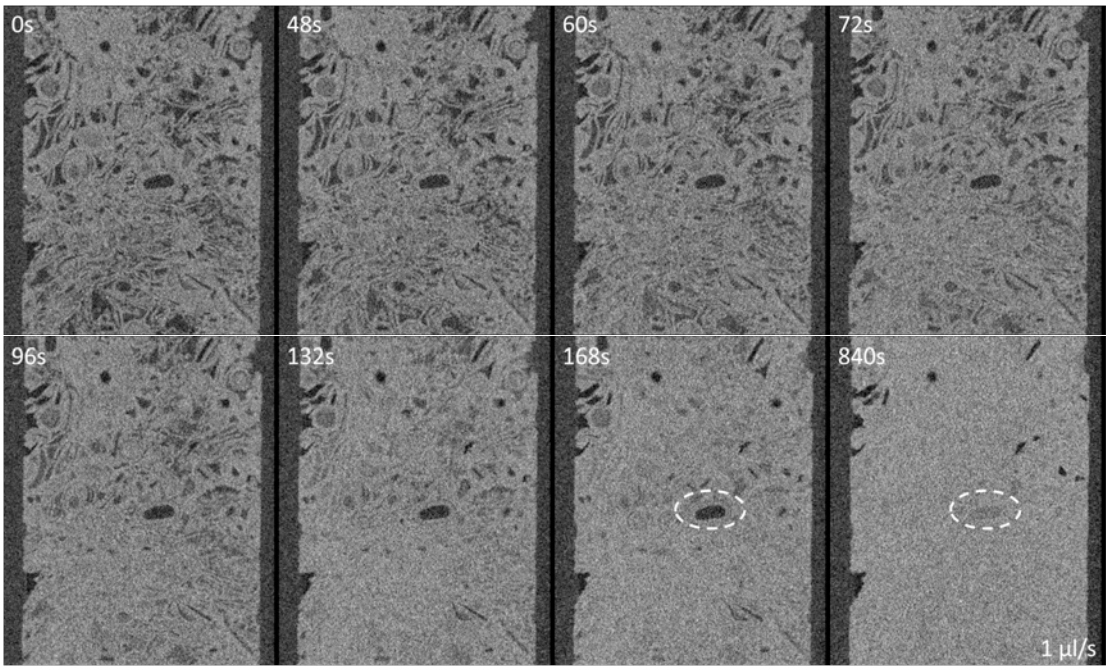

Figure 6. Raw vertical slices through selected reconstructed volume of the continuous acquisition. Experiment at a constant flow speed of 1 µl/s. Dotted circle indicating more isolated, diffusion controlled vuggy porosity.

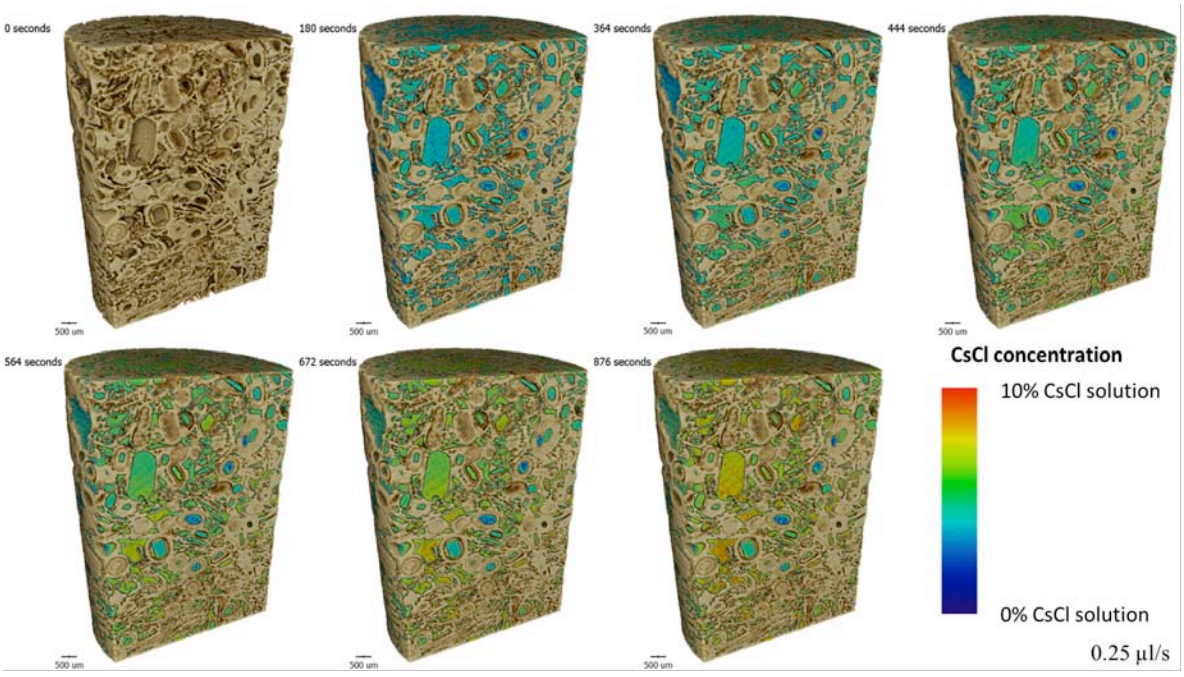

Figure 7. 3D rendering of the CsCl concentration map at different points in time. The concentration in the majority of the pores increases rapidly (rapid change from blue to red), indicating that these pores are well connected and are a part of the preferential flow path of the solute. Other pores remain blue and these are isolated pores controlled by diffusion. Image at 0 seconds showing a rendering of the rock sample without fluid.